International Journal of Nanomedicine

Dovepress
open access to scientific and medical research

Open Access Full Text Article

ORIGINAL RESEARCH

Comparative Colloidal Stability of Commercial Amphotericin B Nanoformulations Using Dynamic and Static Multiple Light Scattering Techniques

Jun Ye[1,2], Renjie Li[1,2], Jialing Cheng[1,2], Dongdong Liu[1,2], Yanfang Yang[1,2], Hongliang Wang[1,2], Xiaoyan Xu[1,2], Lin Li[1,2], Panpan Ma[3], Yuling Liu[1,2]

[1]State Key Laboratory of Bioactive Substance and Function of Natural Medicines, Institute of Materia Medica, Chinese Academy of Medical Sciences & Peking Union Medical College, Beijing, People's Republic of China; [2]Beijing Key Laboratory of Drug Delivery Technology and Novel Formulation, Institute of Materia Medica, Chinese Academy of Medical Sciences & Peking Union Medical College, Beijing, People's Republic of China; [3]Beijing Union Second Pharmaceutical Factory, Beijing, People's Republic of China

Correspondence: Yuling Liu, State Key Laboratory of Bioactive Substance and Function of Natural Medicines, Institute of Materia Medica, Chinese Academy of Medical Sciences & Peking Union Medical College, 1 Xiannongtan Street, Beijing, 100050, People's Republic of China, Tel +86 10-89285188, Fax +86 10-89285190, Email ylliu@imm.ac.cn

Background: Amphotericin B (AmB) nanoformulations have been widely used for the treatment of invasive fungal infections in clinical practice, all of which are lyophilized solid dosage forms that improve storage stability. The colloidal stability of reconstituted lyophilized nanoparticles in an injection medium is a critical quality attribute that directly affects their safety and efficacy during clinical use.

Methods: In the present study, the colloidal stability of commercial AmB nanoformulations, including AmB cholesteryl sulfate complex (AmB-CSC) and AmB liposome (AmB-Lipo), was evaluated using the dynamic (DLS) and static multiple light scattering (SMLS) techniques.

Results: Compared to the DLS technique, the SMLS technique allows for a more objective and accurate evaluation of the colloidal stability of AmB nanoformulations. The results obtained using the SMLS technique demonstrated that AmB-CSC and AmB-Lipo exhibited excellent colloidal stability in both sterile water and 5% dextrose injection. The disk-like structure of the AmB-CSC nanoparticles more readily adsorbed serum proteins to form protein corona compared to the spherical structure of AmB-Lipo after incubation with serum. Additionally, AmB-CSC and AmB-Lipo can significantly reduce the in vitro cytotoxicity and in vivo nephrotoxicity of AmB, which may be attributed to the good colloidal stability and the improved pharmacokinetic profiles of AmB nanoformulations.

Conclusion: To the best of our knowledge, this study is the first to compare the colloidal stability of commercial AmB nanoformulations. These findings will provide useful information not only to inform the clinical use of available AmB nanoformulations but also for improving the design and conduct of translational research on novel AmB nanomedicines.

Keywords: nano-drug delivery systems, colloidal stability, amphotericin B, dynamic light scattering, static multiple light scattering

Introduction

Invasive fungal infections (IFIs) are one of the most common diseases and have become a growing public health concern, posing an important threat to human health.[1,2] Amphotericin B (AmB) is one of the oldest antifungal drugs and remains the gold standard of antifungal therapy because of its broad-spectrum antifungal activity and low incidence of clinical resistance. AmB injection (Fungizone®) is the first marketed AmB formulation, in which sodium deoxycholate is used as a solubilizer to overcome the poor aqueous solubility of AmB.[3] However, intravenous AmB injection is accompanied by a high incidence of nephrotoxicity and infusion-related reactions.[4,5] Nano-drug delivery systems (NDDS) have emerged as promising carriers for improving the therapeutic index and reducing the toxicity of active pharmaceutical ingredients in recent years.[4,6,7] To date, several lipid formulations of AmB based on NDDS have been commercialized to overcome

Received: 30 September 2022
Accepted: 30 November 2022
Published: 6 December 2022

the challenges associated with poor aqueous solubility and nephrotoxicity.[6,8] AmB liposome (AmB-Lipo, AmBisome®), the first injectable NDDS product, is a unilamellar liposome with a nano size, consisting of phospholipids with AmB encapsulated in the bilayer of liposomes. Amphocil®, characterized by a disc-like structure and a particle size of 110–140 nm, is a colloidal dispersion composed of AmB and cholesteryl sodium sulfate at a 1:1 molar ratio.[8,9] AmB cholesteryl sulfate complex (AmB-CSC, Anfulike®) was developed by CSPC Ouyi Pharmaceutical Co., Ltd and approved by the National Medical Products Administration (NMPA) of China in 2021. Additionally, previous studies reported a formulation consisting of a protein-phospholipid bioparticle (Nanodisk), which contained a "super aggregate" form of AmB, exhibited an improved safety profile compared to conventional AmB injection and AmB-Lipo while retaining uncompromised antifungal activities.[5,10] Compared with conventional AmB injection, these lipid nanoformulations exhibited a unique plasma pharmacokinetic profile and decreased the kidney distribution of AmB, which was responsible for the lower incidence of nephrotoxicity.[8,11–13]

As NDDS have been widely explored as tools for biomedical applications, maintaining their stability in physiological environments is one of the main challenges.[14] It is well understood that the physicochemical properties of nanoparticles, including particle size, zeta potential, and colloidal stability, can dictate their biological effects. When introduced into a specific vehicle solution containing electrolytes or proteins, nanoparticles are subjected to several forces that determine their colloidal stability and in vivo behavior.[14,15] Previous studies have confirmed that the poor colloidal stability of nanoformulations in blood circulation directly leads to their poor in vivo performance.[16,17] The predominant form of commercial AmB nanoformulations is a lyophilized yellow powder that must be reconstituted and diluted in a specific vehicle solution before intravenous infusion. In addition, the intravenous infusion should be administered over a period of approximately 2–6 h depending on the dose to reduce infusion-related side effects.[9] Therefore, the colloidal stability of reconstituted nanoparticles within the intravenous infusion period is an important parameter that is directly related to the clinical efficacy and safety of AmB nanoformulations. Thus, a fundamental understanding of the colloidal stability of commercial AmB nanoformulations can provide meaningful insights to facilitate rational clinical medication by elucidating how they behave at systemic levels within biological systems.

Dynamic light scattering (DLS) is a technique used to determine particle size and polydispersity by monitoring time-dependent fluctuations in the intensity of scattered light caused by particle motion.[18] Most studies have evaluated the colloidal stability of nanoparticles by detecting the change in the average particle size and polydispersity of nanoparticles placed at different temperatures for different times using the DLS technique.[19–21] However, DLS can only measure particle size parameters at a specific time point and cannot monitor the dynamic change process of nanoparticles in real time, which does not reflect the real colloidal stability of nanoparticles. Static multiple light scattering (SMLS) has been applied in Turbiscan Tower equipment to detect particle migration and size variations in liquid dispersions.[22] A measurement head moves over the cell height and works with two synchronous detectors, transmission and back-scattering, which offers a highly sensitive and reliable analysis of transparent to opaque samples, even at high concentrations. The transmission and backscattering signals are related to particle size and concentration, and their variation is a sign of destabilization. As the Turbiscan Tower can acquire both destabilization kinetics and mean particle size data of samples without mechanical stress or dilution (concentration up to 95% v/v) at any given time, it has been used to detect at an early stage all kinds of destabilizations, such as coalescence, flocculation, creaming, and sedimentation.[23–28] Therefore, compared with DLS, Turbiscan Tower based on the SMLS technique is a more favorable tool for more accurate and objective evaluation of colloidal stability of nanoparticles placed under different conditions.

Commercial lipid nanoformulations of AmB, such as AmB cholesteryl sulfate complex (AmB-CSC) and AmB liposome (AmB-Lipo), have been widely used for the treatment of IFIs. There is currently a lack of literature evaluating the colloidal stability of reconstituted AmB nanoformulations and providing concrete stable information. In the present study, the colloidal stability of reconstituted AmB nanoformulations, including AmB-Lipo and AmB-CSC, was determined by DLS and SMLS techniques, and further comparative analysis was performed (Figure 1). Additionally, in vitro cytotoxicity and in vivo nephrotoxicity were performed to compare the safety of the reconstituted AmB nanoformulations with that of the conventional AmB formulation. To the best of our knowledge, this is the first study to compare the colloidal stability of the available AmB nanoformulations. This study will provide important information not only for

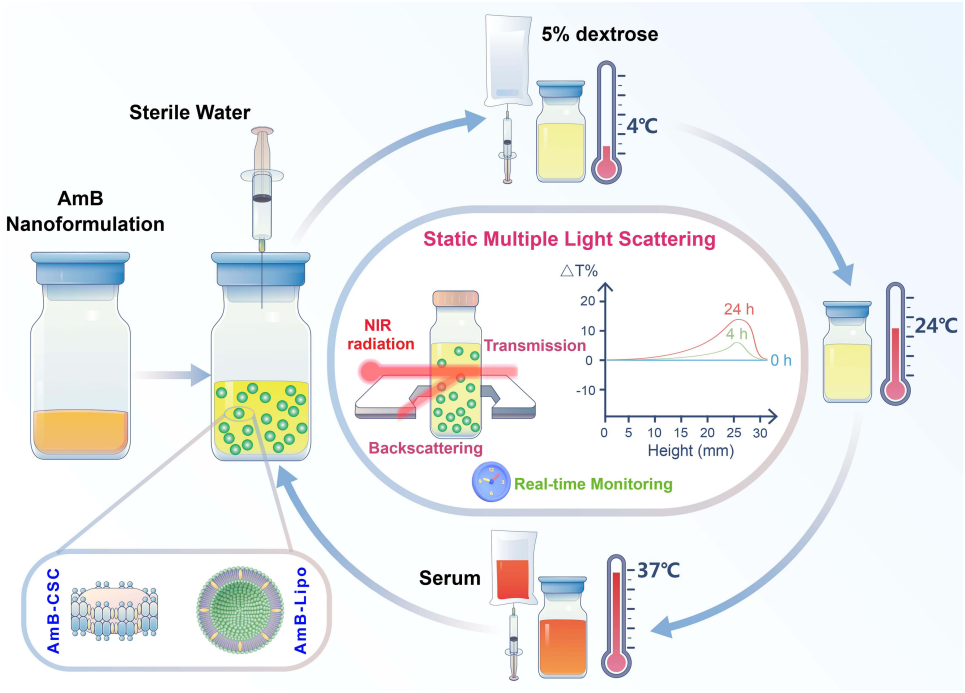

Figure 1 Schematic illustration of comparative colloidal stability of reconstituted commercial amphotericin B nanoformulations at different temperatures for different times using static multiple light scattering technique.

better guiding the clinical use of available AmB nanoformulations but also for improving the design and conduct of translational research on novel AmB nanomedicines.

Materials and Methods

Materials

AmB Cholesteryl Sulfate Complex for Injection was kindly gifted by CSPC Ouyi Pharmaceutical Co., Ltd. (Shijiazhuang, Hebei, China). AmB liposome was obtained from Gilead Sciences Inc. (Foster City, CA, USA). Sterile water for injection was obtained from Cisen Pharmaceutical Co., Ltd. (Jining, Shandong, China). A 5% dextrose injection was obtained from Shijiazhuang Four Pharmaceutical Co., Ltd. (Shijiazhuang, Hebei, China). Fetal bovine serum (FBS) was purchased from ExCell Biotech Co., Ltd. (Shanghai, China).

Cell Culture

Murine RAW264.7 macrophages and human renal tubular duct epithelial cells HK2 were purchased from the Cell Resource Center, Peking Union Medical College (Beijing, China). RAW264.7 macrophages and HK2 cells were cultured in DMEM medium and DMEM/F12 medium, respectively, supplemented with 10% FBS, 100 U/mL penicillin, and 100 μg/mL streptomycin in a humidified atmosphere of 5% CO_2 at 37 °C.

Reconstitution and Dilution of AmB Nanoformulations

Lyophilized powders of AmB nanoformulations, including AmB-CSC and AmB-Lipo, must be reconstituted using sterile water for injection. Briefly, approximately 10 mL of sterile water was aseptically added to each vial for injection to obtain a preparation containing AmB. Immediately after the addition of water, the vial was shaken vigorously for 5 min to completely disperse the AmB nanoformulations, according to the manufacturer's instructions, resulting in the formation of a yellow, translucent suspension. The reconstituted AmB-CSC was taken with a sterile syringe and diluted with 5% dextrose injection to a final concentration of 0.6 mg/mL. It is important to note that the reconstituted AmB-Lipo must be filtered with a 5-micron filter before dilution and the final diluted concentration of AmB was about 1.0 mg/mL.

In vitro Characterization of AmB Nanoformulations

The average particle size, size distribution, polydispersity index (PDI), and zeta potential of the reconstituted AmB nanoformulations were determined by dynamic light scattering (DLS) using a NICOMP 380 ZLS particle sizer (PSS NICOMP, Santa Barbara, CA, USA).[27] Each sample was diluted with 5% dextrose injection, as described above, transferred to a light scattering cell, and analyzed. The analyses were performed at a temperature of 25°C. Each sample was analyzed in triplicate. The average particle size, PDI, and zeta potential values were calculated from the data obtained from at least three cycles. Morphological examination of AmB nanoformulations was performed using transmission electron microscopy (TEM) (JEM1200EX; JEOL, Tokyo, Japan). These nanoparticle suspensions were stained with 2% (w/v) phosphotungstic acid, placed on a carbon film, and observed using TEM.

In vitro Colloidal Stability Using Dynamic Light Scattering (DLS)

The in vitro colloidal stability of reconstituted AmB nanoformulations at 24°C was qualitatively determined by dynamic light scattering (DLS) using a NICOMP 380 ZLS particle sizer. Each sample was diluted with 5% dextrose injection, as described above, and left at 24°C for different periods (0, 2, 4, 8, 12, and 24 h) before transferring to a light scattering cell and analyzed. Each sample was analyzed in triplicate. The average particle size, PDI, and zeta potential of each sample were recorded.

In vitro Colloidal Stability Using Static Multiple Light Scattering (SMLS)

The in vitro colloidal stability of the reconstituted AmB nanoformulations at 4°C or 24°C was qualitatively determined for 24 h using a Turbiscan Tower (Formulaction, L'Union, France) using the static multiple light scattering (SMLS) technique.[26,27] The reconstituted AmB nanoformulations were appropriately diluted as described above and approximately 4 mL of each sample were individually placed in a cylindrical glass cell and stored in the Turbiscan Tower for 24 h at 4 or 24°C. The detection unit of Turbiscan Tower consists of a near-infrared light source (λ = 880 nm) and two synchronous transmission and backscattering detectors. When the detection head scanned the entire cylindrical glass cell, the light passing through the sample (at 180° from the incident beam) or scattering backward by the sample (at 45° from the incident beam) would be captured by transmission or backscattering detectors, respectively. Then, the transmission and backscattering intensity profiles as a function of position were acquired by scanning.[22] The variations in the average transmitted intensity (ΔT) and turbiscan stability index (TSI) calculated from the signal value of transmitted light were used as the main parameters to evaluate the in vitro colloidal stability of AmB nanoformulations.

In vitro Colloidal Stability of AmB Nanoformulations in Serum

To explore the colloidal stability of the diluted AmB nanosuspensions in the blood, FBS was first incubated at 37°C to mimic physiological media. The reconstituted AmB nanoformulations diluted with 5% dextrose injection, as described above, were dispersed in 10% FBS at 37°C. Each sample was incubated in a thermostated air shaker (200 rpm) at 37°C for different periods (0, 2, 4, 8, 12, and 24 h), transferred to a light scattering cell, and analyzed.[29] Each sample was analyzed in triplicate. The average particle size, PDI, and zeta potential of each sample were recorded.

In vitro Cytotoxicity Evaluation of AmB Nanoformulations

The in vitro cytotoxicity of AmB-CSC and AmB-Lipo was evaluated in RAW264.7 macrophages and HK2 cells as compared to the conventional AmB formulation (AmB injection) using CCK-8 kits (Dojindo Laboratories, Tokyo, Japan). RAW264.7 cells and HK2 cells were plated at a density of 2×10^4 and 2×10^3 cells per well in 96-well plates (NEST Biotechnology; Wuxi, Jiangsu, China), respectively. After incubation for 24 h, both RAW264.7 cells and HK2 cells were treated with different AmB samples (AmB injection, AmB-CSC, and AmB-Lipo) containing various concentrations of AmB (0, 0.1, 0.5, 10, 20, and 50 μg/mL). After being treated for 24 h, the number of viable cells was measured using CCK-8 kits, according to the manufacturer's protocol. Untreated cells were used as the control and were considered to be 100% viable.

Nephrotoxicity and Hepatotoxicity of AmB Nanoformulations in vivo

BALB/c mice (female, 6–8 weeks old, 18–20 g) were purchased from Beijing Vital River Laboratory Animal Technology Co., Ltd. (Beijing, China). All animal experiments were approved by the Animal Care and Welfare Committee of the Institute of Materia Medica, Chinese Academy of Medical Sciences & Peking Union Medical College (No. 00003695). The care of laboratory animals and animal experimental operations were performed following the Beijing Administration Rule of Laboratory Animal (2021).[30] The mice (18–20 g) were randomly divided into four groups (control, AmB injection, AmB-CSC, and AmB-Lipo, n = 7 per group) and treated with AmB at the dose of 0.5 mg/kg for 3 days. Serum samples were collected 48 h after the end of dosing. The levels of blood urea nitrogen (BUN) and creatinine (Crea) in serum were determined to evaluate the nephrotoxicity. The levels of alanine aminotransferase (ALT) and aspartate aminotransferase (AST) in serum were measured to assess hepatotoxicity.

Statistical Analysis

All data subjected to statistical analysis were obtained from at least three parallel experiments. Data are presented as the mean ± standard deviation (SD) or mean ± standard error of the mean (SEM). The statistical analysis was performed by Student's t-tests for two groups, and one-way ANOVA for multiple groups using GraphPad Prism version 7.00 for Windows (GraphPad Software, La Jolla, CA, USA). A p-value ≤ 0.05 was considered to be statistically significant.

Results and Discussion

In vitro Characterization of AmB Nanoformulations

IFIs represent a serious threat to public health worldwide.[1,2] AmB has been used as the gold standard of antifungal therapy since its commercialization in the 1950s due to its broad-spectrum antifungal activity and low incidence of clinical resistance.[9] As the traditional AmB formulation poses significant nephrotoxicity, the most widely used antifungal agent in clinical practice is AmB lipid nanoformulations, which could attenuate the nephrotoxic effect of AmB.[6,9]

The colloidal stability of reconstituted nanoformulations is a critical quality attribute that is directly related to clinical efficacy and safety.[16,17,27] A fundamental understanding of the colloidal stability of commercial AmB nanoformulations could provide meaningful insights for their rational clinical use. However, there are no head-to-head studies on the colloidal stability of commercial AmB nanoformulations. In the present study, the comparative colloidal stability of the commercial AmB nanoformulations, AmB Cholesteryl Sulfate Complex (AmB-CSC) and AmB liposome (AmB-Lipo), was determined using DLS and SMLS techniques. First, the physicochemical properties of these AmB nanoformulations, in terms of average particle size and size distribution, PDI, and zeta potential, were characterized by the DLS. DLS is one of the most commonly used techniques to determine the average particle size and particle size distribution of nanoparticles.[31,32] As shown in Figure 2, the predominant form of commercial AmB nanoformulations was a lyophilized yellow lump that needed to be reconstituted in sterile water to form a yellow suspension. Then, the samples were diluted with 5% dextrose injection before determination according to the manufacturer's instructions. As shown in Figure 3, the average particle size of freshly reconstituted AmB-CSC and AmB-Lipo was 137.6 ± 0.8 nm and 131.1 ± 0.5 nm, respectively. TEM revealed roughly spherical and subspherical morphologies of AmB-Lipo, which was consistent with the spherical structure of unilamellar liposomes. The morphology of AmB-CSC was quite different from that of AmB-Lipo, which presented disc-shaped structures under TEM. The average particle size of AmB nanoformulations observed under TEM was consistent with the results determined by the DLS. Compared to AmB-Lipo, AmB-CSC showed an evident tendency for aggregation, which was also seen in a previously published study.[10] As shown in Figure 4, AmB-CSC and AmB-Lipo displayed low PDI values (<0.2), indicating narrow size distributions of these nanoformulations. The zeta potential is a function of the particle surface charge, which is a key indicator for estimating the colloidal stability of nanosuspensions.[32,33] It is commonly accepted that a high zeta potential, in which the absolute value is above 30 mV, could provide an electrostatic repulsion to prevent nanoparticles aggregation.[32] The greater the absolute value of the zeta potential, the more stable the nanosuspension. The zeta potential of freshly reconstituted AmB-CSC and AmB-Lipo was −40.0 ± 0.3 mV and −48.5 ± 1.5 mV, respectively (Figure 4), which indicates that these AmB nanoformulations may have good colloidal stability when dispersed in 5% dextrose injection.

Figure 2 Appearance of commercial AmB nanoformulations including AmB-CSC (**A**) and AmB-Lipo (**B**) before and after reconstitution with sterile water.
Abbreviations: AmB, amphotericin B; AmB-CSC, AmB cholesteryl sulfate complex; AmB-Lipo, AmB liposome.

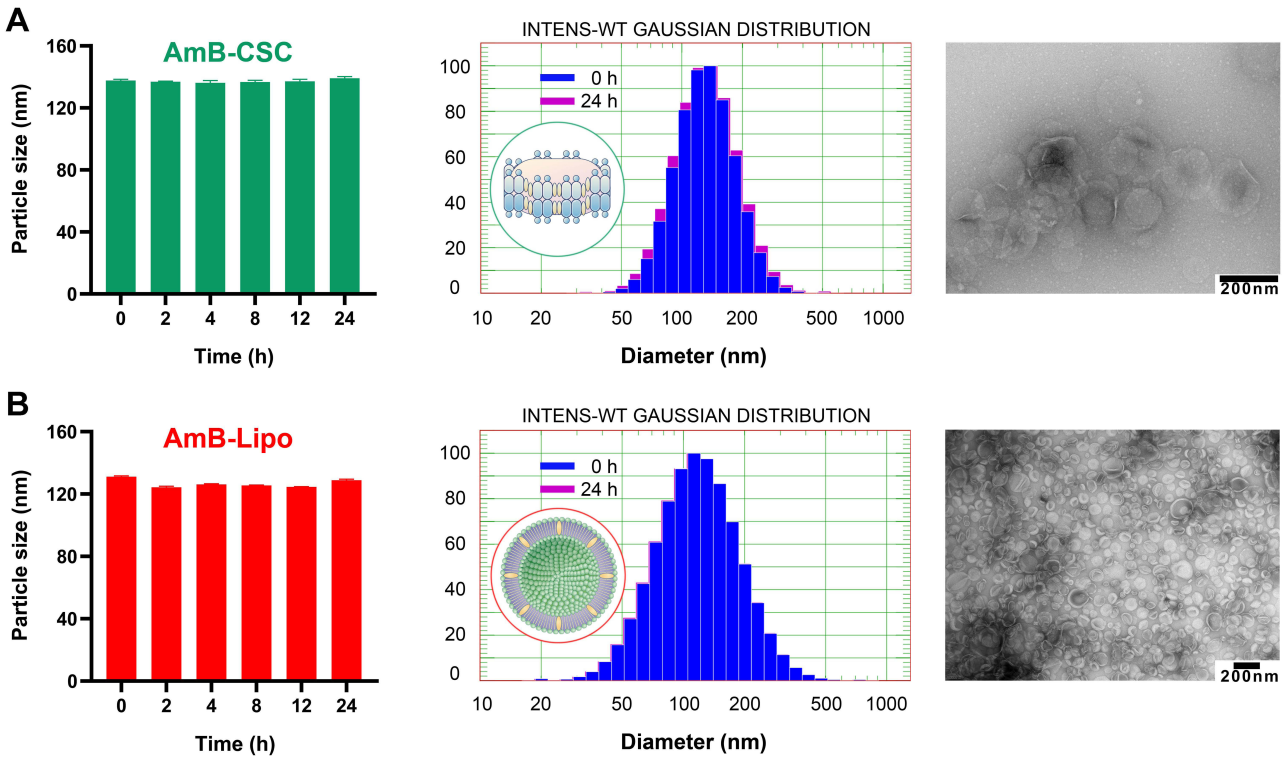

Figure 3 In vitro characterization of AmB nanoformulations. Average particle size, particle size distribution, and TEM images of AmB-CSC (**A**) and AmB-Lipo (**B**). Each value represents the mean ± SD (n = 3).
Abbreviations: AmB, amphotericin B; TEM, transmission electron microscopy; AmB-CSC, AmB cholesteryl sulfate complex; AmB-Lipo, AmB liposome; SD, standard deviation.

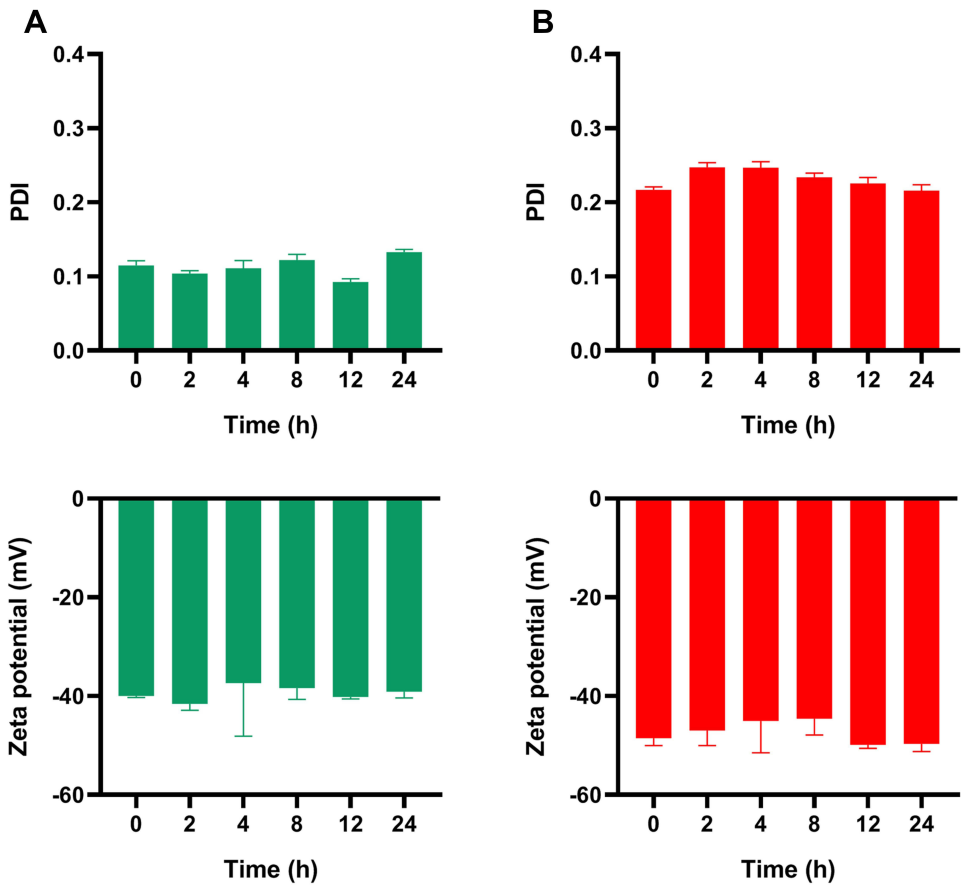

Figure 4 PDI and zeta potential of AmB-CSC (**A**) and AmB-Lipo (**B**). Each value represents the mean ± SD (n = 3).
Abbreviations: PDI, polydispersity index; AmB, amphotericin B; AmB-CSC, AmB cholesteryl sulfate complex; AmB-Lipo, AmB liposome; SD, standard deviation.

In vitro Colloidal Stability Using the DLS Technique

DLS is the most widely applied technique for measuring the particle size distribution and PDI of nanosuspensions.[18] Herein, the colloidal stability of the nanosuspension was evaluated indirectly in comparison with the change in average particle size and PDI of nanoparticles placed at different temperatures for different times.[19,21,34] However, certain disadvantages are associated with this method. For example, the samples were shaken and mixed well before each determination. The flocculated nanoparticles were re-dispersed in the medium after shaking and mixing, and the average particle size and particle size distribution hardly changed in a short time, which led to false-positive results.[27] In addition, the method is limited by the concentration of nanoparticles: samples that are too thick or too thin will affect the accuracy of the determination results.[18,24]

To investigate the properties of the nanoformulations on temporal scales, the average particle size, PDI, and zeta potential were monitored by DLS at specific time points (0, 2, 4, 8, 12, and 24 h). As shown in Figures 3 and 4, the average particle size, size distribution, and zeta potential of the AmB nanoformulations hardly changed with time within 24 h at 24°C. However, this result did not fully prove that these AmB nanoformulations had good colloidal stability owing to the certain deficiencies of the DLS technique described above. Therefore, a more accurate method is needed to further evaluate the colloidal stability of AmB nanoformulations.

In vitro Colloidal Stability Using the SMLS Technique

Because particles or droplets are in weak equilibrium within the liquid phase, it is important to analyze their dispersion state in the native form. Optical methods, such as DLS, which require sample dilution, offer limited possibilities for analyzing samples in the native form.[18] SMLS is the most suitable optical method for directly characterizing

nanodispersions without dilution or the perturbation of their initial form. The actual dispersion state, such as the presence of agglomerates or flocs, can be rapidly and precisely identified and measured without altering the actual particle size. Therefore, SMLS offers a more accurate determination of the physical phenomena occurring over time.[24] To further characterize the colloidal stability of AmB nanoformulations, Turbiscan Tower based on the SMLS technique was used to precisely monitor the variation in the relative stability of the transmitted light, which could detect early imperceptible changes before the appearance of macroscopic physical modifications in nanoparticles.[26,27]

Two steps were required to prepare the lyophilized AmB nanoformulations. The lyophilized clump was dissolved in an appropriate amount of sterile water. The concentrated nanodispersions were then diluted to specific concentrations in 5% dextrose injection for infusion administration. First, the colloidal stability of these concentrated AmB nanodispersions was assessed using Turbiscan Tower at 24°C for 24 h. The variation in droplet volume fraction or size was evident as a variation in the light transmission (ΔT) profiles. When the variation was >10%, the nanodispersion system was unstable.[26] As shown in Figure S1, the variations in the transmission profiles (ΔT) of these concentrated AmB nanodispersions were <10%, indicating no apparent aggregation or sedimentation upon dispersion of these nanoformulations in sterile injection water at 24°C for 24 h. The Turbiscan Stability Index (TSI) is a one-click parameter calculated from the changes in transmitted light to easily compare the colloidal stability of samples in a kinetic manner. The higher the TSI, the less stable the nanodispersions.[25,26] Although the TSI of these AmB nanoformulations increased slowly over time, they remained at a low level (TSI <1.0). These results indicate that these concentrated AmB nanodispersions possess favorable colloidal stability, which may be attributed to their highly negative zeta potential.

Second, the colloidal stability of the diluted AmB nanodispersions was assessed using Turbiscan Tower at 4°C or 24°C for 24 h. Because the diluted AmB nanodispersions are ultimately used for intravenous infusion, their colloidal stability is critical for clinical use. At 4°C, the ΔT of diluted AmB-CSC and AmB-Lipo were very low (<1%), demonstrating that AmB-CSC and AmB-Lipo dispersed in 5% dextrose injection exhibited excellent stability at 4°C for 24 h. Except for ΔT, the value of TSI also exhibited a similar feature of colloidal stability. The TSI of diluted AmB-CSC and AmB-Lipo only changed negligibly and remained at a very low level (<0.3) (Figure 5). Compared with the samples at 4°C, the ΔT of diluted AmB-CSC and AmB-Lipo was higher at 24°C; however, the values were relatively low (<5%), suggesting that AmB-CSC and AmB-Lipo dispersed in 5% dextrose injection exhibited good stability at 24°C for 24 h. The TSI of diluted AmB-CSC and AmB-Lipo increased slowly over time but did not exceed 1.0 after 24 h (Figure 6). As these AmB nanodispersions are thermodynamically unstable colloidal dispersion systems, their colloidal stability is reduced by increasing the temperature from 4°C to 24°C.

Although the average particle size and PDI of these AmB nanoformulations remained almost unchanged over time at 24°C within 24 h (Figure 3), there is a difference in their colloidal stability based on the results obtained from the Turbiscan Tower (Figure 6). AmB-CSC dispersed in 5% dextrose injection exhibited better colloidal stability than AmB-Lipo at 24°C, as evidenced by the lower TSI of AmB-CSC. In our previous study, commercial paclitaxel nanoformulations, including paclitaxel nanoparticles (albumin-bound) and paclitaxel liposomes, exhibited no obvious change in particle size distribution using DLS but different colloid stability using SMLS.[27] Compared with the determination of average particle size and PDI by DLS, the ΔT and TSI values obtained using the SMLS technique allow for a more objective and accurate evaluation of the colloidal stability of AmB nanoformulations. The favorable colloidal stability of AmB-CSC and AmB-Lipo may be attributed to their smaller particle size (< 150 nm) and highly negative zeta potential (< −40 mV) and/or steric hindrance.

It has been pointed out that electrostatic repulsion, steric hindrance and/or electrostatic repulsion are the main repulsive force preventing the aggregation and fusion of lipid bilayer fragments and nanodisks in a dispersion medium.[35] Hydrophobic drugs have been shown to distribute into the rim of electrostatically stable lipid fragments and the sterically stabilized nanodisks may be applied in a similar way to enhance the solubility of insoluble drugs.[36] In addition, the colloidal stability and particle size of nanodisks can be further improved by regulating the amount of hydrophilic polymer PEGylated phospholipids in the lipid materials.[36–38]

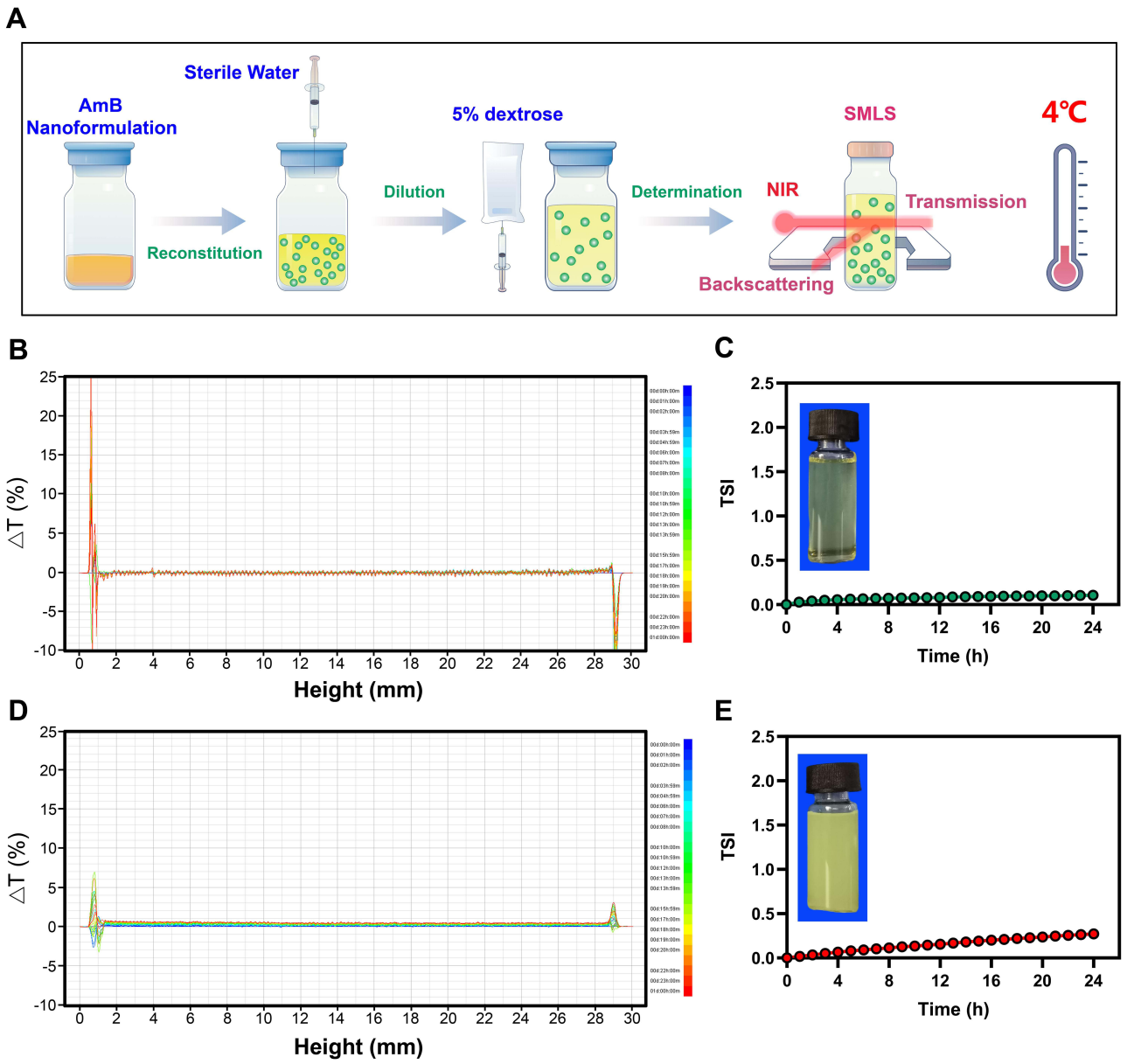

Figure 5 In vitro colloidal stability of the diluted AmB nanodispersions at 4°C for 24 h. (**A**) Schematic illustration of the measurement process. Variations of transmission profiles (ΔT) and TSI of AmB-CSC (**B** and **C**) and AmB-Lipo (**D** and **E**) diluted in 5% dextrose injection at 4°C for 24 h.
Abbreviations: AmB, amphotericin B; TSI, turbiscan stability index; AmB-CSC, AmB cholesteryl sulfate complex; AmB-Lipo, AmB liposome.

The Colloidal Stability of AmB Nanoformulations in Serum

After reconstitution and dilution with 5% dextrose injection, AmB nanoformulation is injected intravenously. Once injected into the bloodstream environment, nanoparticles interface with a wide range of biomacromolecules, particularly serum proteins.[15] Upon contact with serum proteins, non-specific proteins bind rapidly to the surface of nanoparticles, forming a protein corona, leading to changes in the surface properties that have been shown to play a critical role in the determination of subsequent physiological behavior.[29,39,40] Thus, it is pivotal to explore nanoparticles' properties and, more importantly, colloidal behavior in biological solutions, which will determine their biodistribution, pharmacokinetics, and systemic toxicity in vivo.[15] In the present study, the colloidal stability of diluted AmB nanodispersions dispersed in 10% FBS was evaluated by detecting the change in the average particle size and PDI at specific time points by DLS. Because blood flows, the colloidal stability of diluted AmB nanodispersions in a fluid containing FBS that mimics blood is unsuitable for evaluation using the SMLS technique.

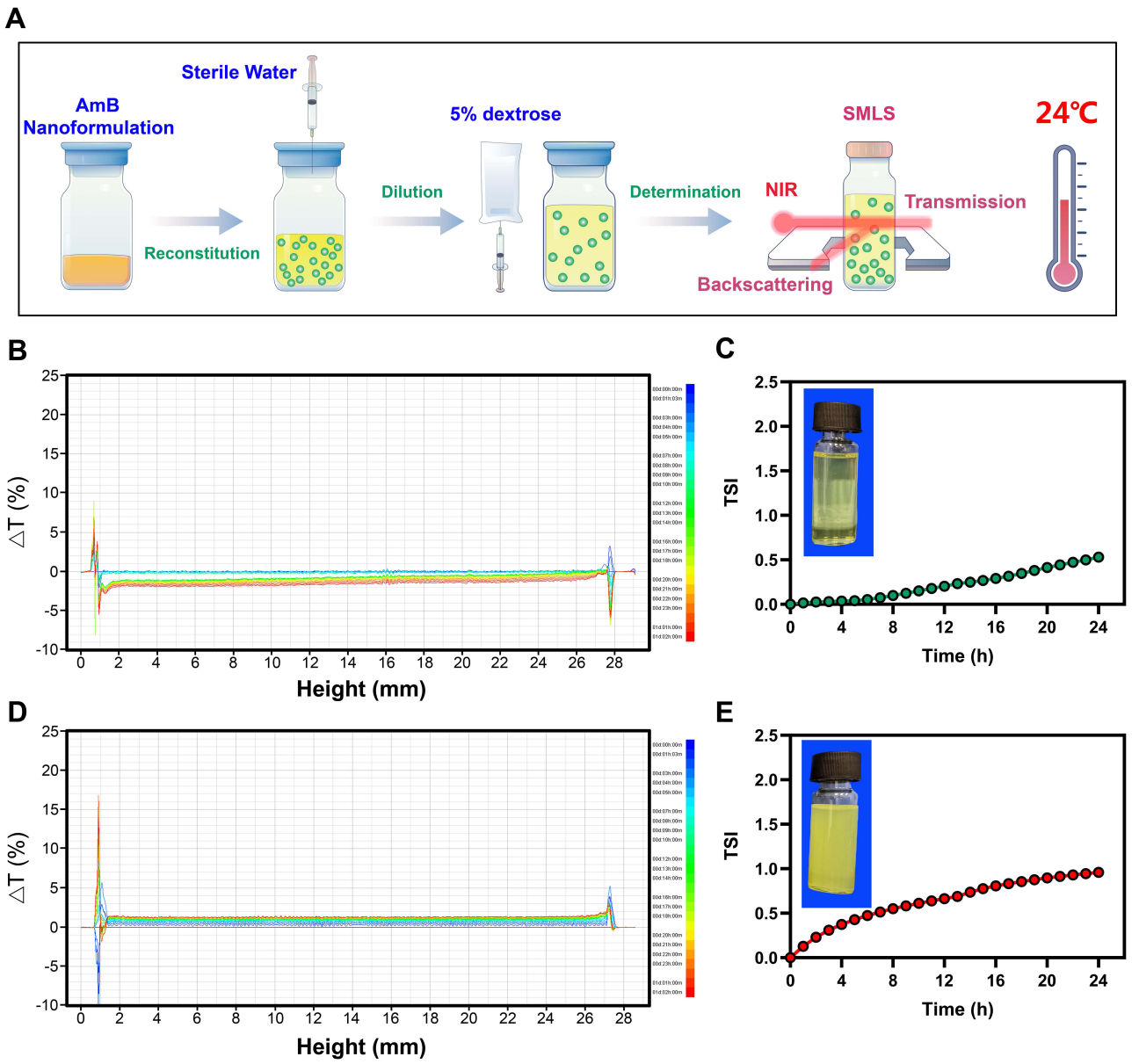

Figure 6 In vitro colloidal stability of the diluted AmB nanodispersions at 24°C for 24 h. (**A**) Schematic illustration of the measurement process. Variations of transmission profiles (ΔT) and TSI of AmB-CSC (**B** and **C**) and AmB-Lipo (**D** and **E**) diluted in 5% dextrose injection at 24°C for 24 h.
Abbreviations: AmB, amphotericin B; TSI, turbiscan stability index; AmB-CSC, AmB cholesteryl sulfate complex; AmB-Lipo, AmB liposome.

As shown in Figure 7, the average particle size of the AmB-CSC nanodispersions increased from 145.1 ± 1.1 nm to 238.6 ± 1.4 nm immediately after dispersion with FBS. Subsequently, its average particle size gradually decreases with time and is restored to the initial level. Similar to the average particle size, the PDI of the AmB-CSC nanodispersions exhibited the same trend. In contrast, the average particle size and PDI of the AmB-Lipo did not change significantly over time after incubation with 10% FBS. These results suggest that the AmB-CSC nanodispersions were more strongly affected by the components in FBS than AmB-Lipo. This may be due to the disk-like structure of the AmB-CSC nanoparticles more readily adsorbing serum proteins to form protein corona compared to the spherical structure of AmB-Lipo.[41] Although the average particle size of the AmB-CSC nanoparticles increased rapidly when mixed with serum proteins, it subsequently decreased during the incubation period. This phenomenon may be attributed to the dynamic reversible change in the association and dissociation of protein coronas on the surfaces of the nanoparticles during incubation. These results are also in line with a previous study in which the adsorption and desorption of protein coronas

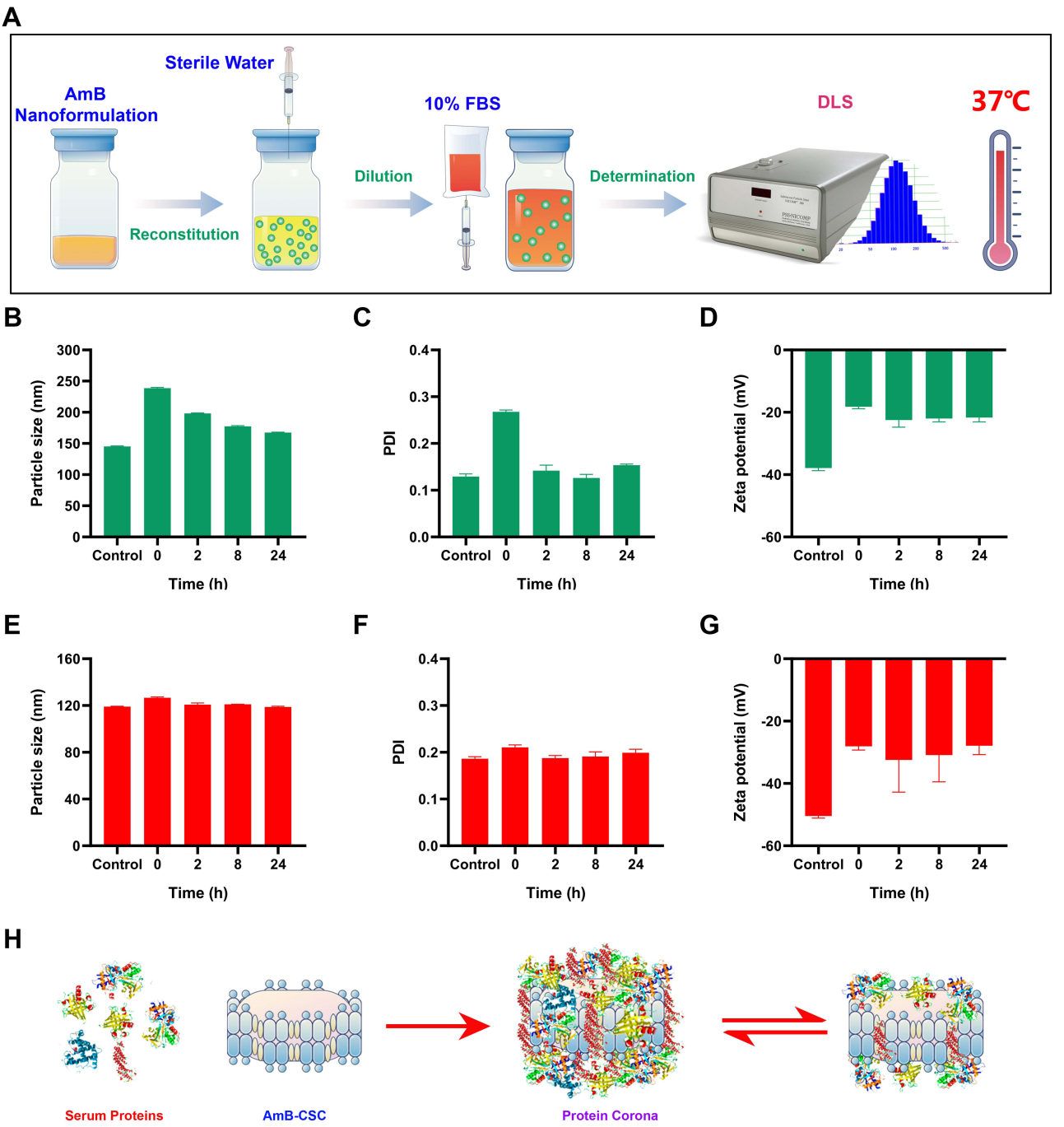

Figure 7 The colloidal stability of AmB nanoformulations in 10% FBS at 37°C for 24 h. (**A**) Schematic illustration of the measurement process. Average particle size, PDI, and zeta potential of diluted AmB-CSC (**B-D**) and AmB-Lipo (**E-G**) nanodispersions incubated with 10% FBS at 37°C for 24 h. (**H**) The protein corona on the surfaces of AmB-CSC nanoparticles during incubation with FBS. Each value represents the mean ± SD (n = 3).

Abbreviations: AmB, amphotericin B; FBS, fetal bovine serum; PDI, polydispersity index; AmB-CSC, AmB cholesteryl sulfate complex; AmB-Lipo, AmB liposome; SD, standard deviation.

occurred after nanoparticles entered the blood.[29] To further investigate the nanoparticle–protein interactions, the zeta potential was also determined, which is an important parameter that affects the formation of protein coronas. Upon contact with FBS, the zeta potential of these AmB nanodispersions decreased in absolute value (became less negative) and then remained relatively stable over time. The change characteristic of the zeta potential in this study is consistent with previously published literature.[40] Previous studies have reported that the effect of FBS on the colloidal stability of several types of nanoparticles depends on their composition, surface chemistry, and particle size.[39] In our current study,

AmB-CSC nanodispersions interacted more readily with the components in FBS than AmB-Lipo, indicating that the composition and shape of nanoparticles play a major role. Preceding reports have revealed that the surface properties of nanocarriers including shape, size, charge, and surface modifications have a significant influence on the formation of protein coronas.[42–44] Shape is one of the critical parameters affecting the formation of protein coronas, which changes the curvature of nanocarriers. The composition of nanocarriers regulates the protein coronas mainly through the surface charge and steric hindrance of materials.[42] A previous study reported that the special discoid morphology of lipid nanodiscs dramatically changed the protein pattern adsorbed on the nanocarrier surface as compared to spherical liposomes: nanodiscs were more likely to adsorb apolipoproteins whereas spherical liposomes mainly adsorbed albumin.[44] The apolipoproteins adsorbed on the surface of the nanodiscs could act as membrane scaffold proteins to improve their colloidal stability, prolong their blood circulation, and improve biocompatibility.[45,46] However, the impact of the protein corona surrounded by the surface of the AmB-CSC nanoparticles on the biological behavior in vivo requires further evaluation.

Reconstituted AmB Nanoformulations Reduced AmB Cytotoxicity

AmB binds to ergosterol in the fungal membrane to form pores, which causes the efflux of ions within the fungus and eventually leads to the death of the fungus. However, AmB can also bind to cholesterol in mammalian cell membranes and thus damage normal cells.[47,48] The first marketed AmB formulation is AmB injection, in which sodium deoxycholate is used as a solubilizer to dissolve AmB. However, intravenous AmB injection is accompanied by a high incidence of nephrotoxicity and infusion-related reactions.[5,6] The high incidence of nephrotoxicity induced by AmB injection is attributed to the high distribution of AmB in renal tissue and the binding of AmB to the cholesterol of cell membrane in renal tissue. Accumulated evidence confirmed that nanoformulations have multiple advantages over conventional delivery systems, such as improved in vivo pharmacokinetic profile and enhanced safety. To compare the in vitro cytotoxicity of the reconstituted AmB nanoformulations (AmB-CSC and AmB-Lipo) with that of the conventional AmB formulation (AmB injection), the human renal tubular duct epithelial cells HK2 and murine RAW264.7 macrophages were treated with three AmB formulations and the cell viability was determined.

The results of in vitro cytotoxicity demonstrated that AmB injection produced significant cytotoxicity to HK2 cells when the concentration of AmB was higher than 0.1 μg/mL, and only approximately 44% of HK2 cells survived when the concentration was increased to 50 μg/mL (Figure 8A and B). Comparatively, the survival rate of HK2 cells after treatment with reconstituted AmB nanoformulations (AmB-CSC and AmB-Lipo) at AmB concentrations of 0.1–50 μg/mL was near 100% (Figure 8C and D), indicating negligible cytotoxicity of reconstituted AmB nanoformulations to human renal tubular duct epithelial cells. The encapsulation effect of AmB by nanoparticles leads to the inability of AmB to bind to cholesterol on the cell membrane, which is responsible for the reduced cytotoxicity of AmB nanoformulations (Figure 8E). Similar in vitro cytotoxicity results were also verified in RAW264.7 macrophages (Figure 9). It is noteworthy that AmB nanoformulations can significantly promote macrophage proliferation when incubated with high concentrations, which may be related to the strong phagocytosis of macrophages to nanoparticles. In addition, the above results can also indirectly confirm that the integrity of AmB nanoparticles after reconstitution can still be maintained when dispersed in a cell culture medium for 24 h. This is also consistent with the in vitro colloidal stability results described above.

Reconstituted AmB Nanoformulations Reduced in vivo Nephrotoxicity of AmB

Although AmB is the gold standard for the clinical treatment of IFIs, the nephrotoxicity induced by conventional AmB injection seriously limits its clinical application. To further compare the in vivo nephrotoxicity of the reconstituted AmB nanoformulations (AmB-CSC and AmB-Lipo) with that of the conventional AmB formulation (AmB injection), the mice were administered with three AmB formulations, and the serum biochemical indicators related to the liver and kidney function was determined. As shown in Figure 10, the treatment of AmB injection significantly increased the levels of BUN and Crea in serum compared to the control group. Comparatively, there was no significant changes were observed in the serum BUN and Crea levels of the reconstituted AmB nanoformulations (AmB-CSC and AmB-Lipo) groups compared to that of the control group. These results indicated that AmB

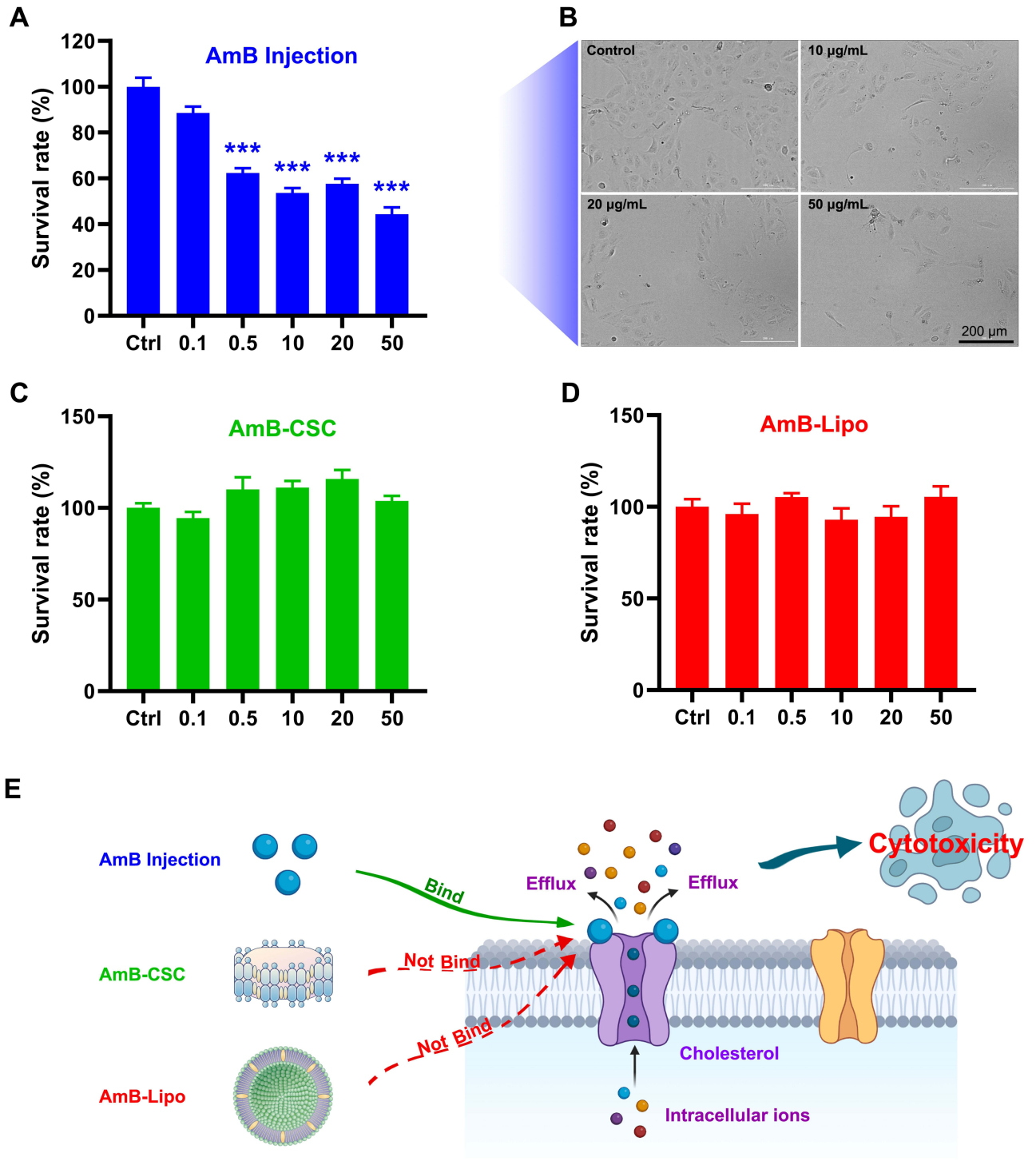

Figure 8 In vitro cytotoxicity of AmB injection, AmB-CSC, and AmB-Lipo in human renal tubular duct epithelial cells HK2. The HK2 cells were treated with AmB injection (**A**), AmB-CSC (**C**), and AmB-Lipo (**D**) at AmB concentrations of 0.1–50 μg/mL for 24 h and the cell viability was determined using CCK-8 kits. Each value represents the mean ± SEM (n = 6). ***p < 0.001 compared with the control (Ctrl) group. The cell morphology of HK2 cells after incubation with AmB injection (**B**) was observed by Cell Imaging Multimode Reader (Cytation 5, BioTek). AmB binds to cholesterol in the cell membrane to form pores, which causes the efflux of intracellular ions and eventually leads to cell death (**E**).

Abbreviations: AmB, amphotericin B; AmB-CSC, AmB cholesteryl sulfate complex; AmB-Lipo, AmB liposome; SEM, standard error of the mean.

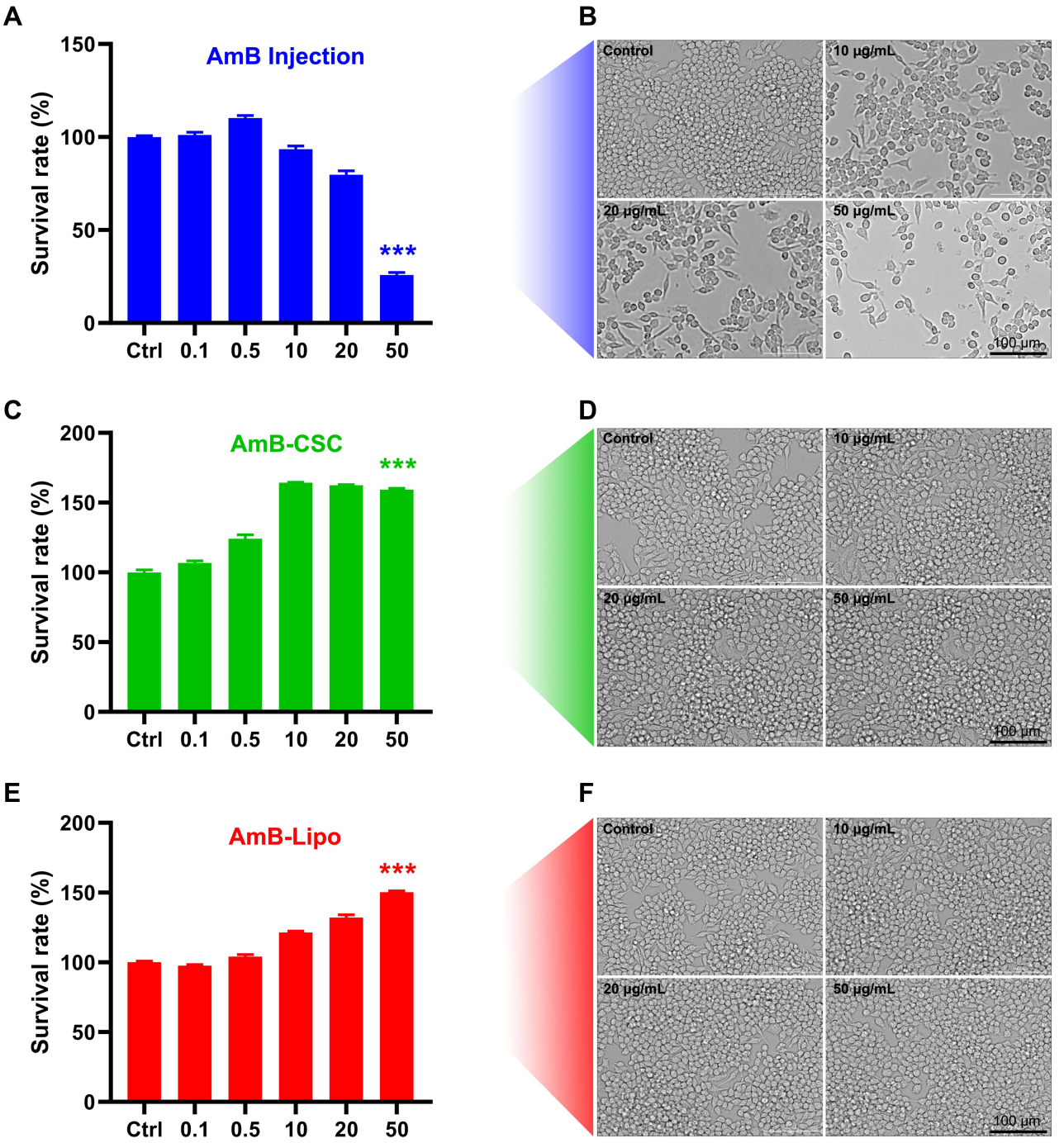

Figure 9 In vitro cytotoxicity of AmB injection, AmB-CSC, and AmB-Lipo in murine RAW264.7 macrophages. The murine RAW264.7 macrophages were treated with AmB injection (**A**), AmB-CSC (**C**), and AmB-Lipo (**E**) at AmB concentrations of 0.1–50 μg/mL for 24 h and the cell viability was determined using CCK-8 kits. Each value represents the mean ± SEM (n = 6). ***p < 0.001 compared with the control (Ctrl) group. The cell morphology of RAW264.7 macrophages after incubation with AmB injection (**B**), AmB-CSC (**D**), and AmB-Lipo (**F**) was observed by Cell Imaging Multimode Reader (Cytation 5, BioTek).
Abbreviations: AmB, amphotericin B; AmB-CSC, AmB cholesteryl sulfate complex; AmB-Lipo, AmB liposome; SEM, standard error of the mean.

nanoformulations (AmB-CSC and AmB-Lipo) can significantly reduce the in vivo nephrotoxicity of AmB, which may be attributed to the good colloidal stability and the improved pharmacokinetic profiles of AmB nanoformulations.[47,49] In the present study, AmB-CSC were more readily adsorbing serum proteins to form protein corona compared to AmB-Lipo, while there was no significant difference between AmB-CSC and AmB-Lipo for in vivo nephrotoxicity. The reason behind this phenomenon is very likely the dynamic reversible change in the association and dissociation of

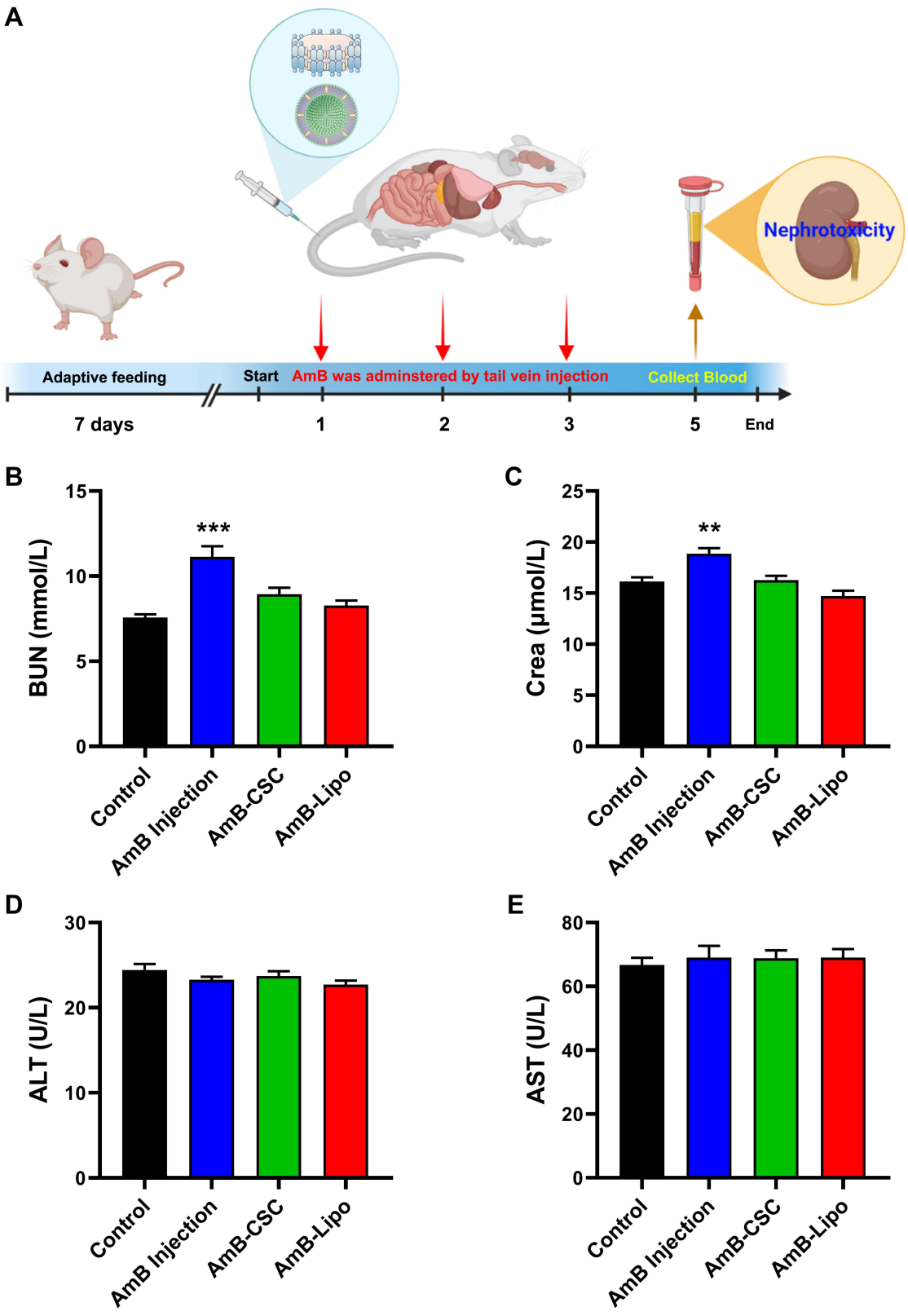

Figure 10 In vivo nephrotoxicity and hepatotoxicity of AmB nanoformulations as compared to conventional AmB injection. (**A**) Schematic illustration of the administration and serum samples collection process. The determination of blood biochemistry parameters including BUN (**B**), Crea (**C**), ALT (**D**), and AST (**E**) levels. After 48 h administration of AmB injection, AmB-CSC, and AmB-Lipo to female BALB/c mice at a dose of 0.5 mg/kg, serum samples were collected and biochemical parameters were determined. Each value represents the mean ± SEM (n = 7). **p < 0.01, ***p < 0.001 compared with the control group.

Abbreviations: AmB, amphotericin B; BUN, blood urea nitrogen; Crea, creatinine; ALT, alanine aminotransferase; AST, aspartate aminotransferase; AmB-CSC, AmB cholesteryl sulfate complex; AmB-Lipo, AmB liposome; SEM, standard error of the mean.

protein coronas on the surfaces of AmB-CSC during incubation, which was preliminarily confirmed by the change in the particle size. However, the deeper mechanisms need to be explored in our future experiments.

Conclusions

The present study was designed with the aim of exploring the colloidal stability of commercial AmB nanoformulations dispersed in sterile water and 5% dextrose injection by DLS and SMLS for 24 h. The results demonstrated that the AmB-CSC and AmB-Lipo exhibited good colloidal stability in both sterile water and 5% dextrose injection at 4°C or 24°C for 24 h. Compared with the DLS technique, the SMLS technique allows for a more objective and accurate evaluation of the colloidal stability of AmB nanoformulations. The favorable colloidal stability of AmB-CSC and AmB-Lipo may be attributed to their small particle size and highly negative zeta potential. Moreover, the disk-like structure of the AmB-CSC nanoparticles more readily adsorbed serum proteins to form protein corona compared to the spherical structure of AmB-Lipo. However, two main limitations of this study are that the release characteristics of AmB-CSC and AmB-Lipo under different release conditions and the species and mechanisms of AmB-CSC adsorbing serum proteins to form protein corona in serum were not investigated. Additionally, AmB-CSC and AmB-Lipo can significantly reduce the in vitro cytotoxicity and in vivo nephrotoxicity of AmB, which may be attributed to the good colloidal stability and the improved pharmacokinetic profiles of AmB nanoformulations. These findings provide useful information not only to inform the clinical use of available AmB nanoformulations but also to improve the design and conduct of translational research on novel AmB nanomedicines.

Acknowledgments

This work was financially supported by the National Science and Technology Major Project of China (2018ZX09711001), Beijing Nova Program (Z211100002121127), Beijing Natural Science Foundation (L212059), Fundamental Research Funds for the Central Universities (3332021101), and CAMS Innovation Fund for Medical Sciences (CIFMS, 2022-I2M-JB-011). We thank CSPC Ouyi Pharmaceutical Co., Ltd for providing the study drugs.

Disclosure

The authors declare no conflicts of interest in this work.

References

1. Pathakumari B, Liang G, Liu W. Immune defence to invasive fungal infections: a comprehensive review. *Biomed Pharmacother*. 2020;130:110550. doi:10.1016/j.biopha.2020.110550
2. Enoch DA, Yang H, Aliyu SH, Micallef C. The Changing Epidemiology of Invasive Fungal Infections. *Methods Mol Biol*. 2017;1508:17–65. doi:10.1007/978-1-4939-6515-1_2
3. Kaur L. Safe and Effective Delivery of Amphotericin B: a Survey of Patents. *Recent Pat Nanotechnol*. 2017;11:214–234. doi:10.2174/1872210511666170105130210
4. Jafari M, Abolmaali SS, Tamaddon AM, Zomorodian K, Sarkari BS. Nanotechnology approaches for delivery and targeting of Amphotericin B in fungal and parasitic diseases. *Nanomedicine*. 2021;16:857–877. doi:10.2217/nnm-2020-0482
5. Faustino C, Pinheiro L. Lipid Systems for the Delivery of Amphotericin B in Antifungal Therapy. *Pharmaceutics*. 2020;12. doi:10.3390/pharmaceutics13010012
6. Wang X, Mohammad IS, Fan L, et al. Delivery strategies of amphotericin B for invasive fungal infections. *Acta Pharm Sin B*. 2021;11:2585–2604. doi:10.1016/j.apsb.2021.04.010
7. Ma Z, Wang X, Li C. Strategies of Drug Delivery for Deep Fungal Infection: a Review. *Pharm Nanotechnol*. 2020;8:372–390. doi:10.2174/2211738508666200910101923
8. Zaioncz S, Khalil NM, Mainardes RM. Exploring the role of nanoparticles in amphotericin B delivery. *Curr Pharm Des*. 2017;23:509–521. doi:10.2174/1381612822666161027103640
9. Fernández-García R, de Pablo E, Ballesteros MP, Serrano DR. Unmet clinical needs in the treatment of systemic fungal infections: the role of amphotericin B and drug targeting. *Int J Pharm*. 2017;525:139–148. doi:10.1016/j.ijpharm.2017.04.013
10. Burgess BL, He Y, Baker MM, et al. NanoDisk containing super aggregated amphotericin B: a high therapeutic index antifungal formulation with enhanced potency. *Int J Nanomedicine*. 2013;8:4733–4743. doi:10.2147/IJN.S50113
11. Huang ZW, Yu JC, Wang JJ, et al. Pharmacokinetics and Safety of Single-Dose Amphotericin B Colloidal Dispersion in Healthy Chinese Subjects and Population Pharmacokinetic/Pharmacodynamic Analysis to Inform Clinical Efficacy in Invasive Infections Caused by Candida albicans. *Clin Ther*. 2021;43:1921–1933.e1927. doi:10.1016/j.clinthera.2021.09.012
12. Aversa F, Busca A, Candoni A, et al. Liposomal amphotericin B (AmBisome®) at beginning of its third decade of clinical use. *J Chemother*. 2017;29:131–143. doi:10.1080/1120009X.2017.1306183

13. Groll AH, Rijnders BJA, Walsh TJ, Adler-Moore J, Lewis RE. Clinical Pharmacokinetics, Pharmacodynamics, Safety and Efficacy of Liposomal Amphotericin B. *Clin Infect Dis*. 2019;68:S260–s274. doi:10.1093/cid/ciz076
14. Rabel M, Warncke P, Thürmer M, et al. The differences of the impact of a lipid and protein Corona on the colloidal stability, toxicity, and degradation behavior of iron oxide nanoparticles. *Nanoscale*. 2021;13:9415–9435. doi:10.1039/D0NR09053K
15. Moore TL, Rodriguez-Lorenzo L, Hirsch V, et al. Nanoparticle colloidal stability in cell culture media and impact on cellular interactions. *Chem Soc Rev*. 2015;44:6287–6305. doi:10.1039/C4CS00487F
16. Ruttala HB, Ramasamy T, Shin BS, Choi HG, Yong CS, Kim JO. Layer-by-layer assembly of hierarchical nanoarchitectures to enhance the systemic performance of nanoparticle albumin-bound paclitaxel. *Int J Pharm*. 2017;519:11–21. doi:10.1016/j.ijpharm.2017.01.011
17. Ruttala HB, Ko YT. Liposome encapsulated albumin-paclitaxel nanoparticle for enhanced antitumor efficacy. *Pharm Res*. 2015;32:1002–1016. doi:10.1007/s11095-014-1512-2
18. Bhattacharjee S. DLS and zeta potential - What they are and what they are not? *J Control Release*. 2016;235:337–351. doi:10.1016/j.jconrel.2016.06.017
19. Chiu-Lam A, Staples E, Pepine CJ, Rinaldi C. Perfusion, cryopreservation, and nanowarming of whole hearts using colloidally stable magnetic cryopreservation agent solutions. *Sci Advances*. 2021;7:eabe3005. doi:10.1126/sciadv.abe3005
20. Pelaz B, Del Pino P, Maffre P, et al. Surface functionalization of nanoparticles with polyethylene glycol: effects on protein adsorption and cellular uptake. *ACS Nano*. 2015;9:6996–7008. doi:10.1021/acsnano.5b01326
21. Ashkbar A, Rezaei F, Attari F, Ashkevarian S. Treatment of breast cancer in vivo by dual photodynamic and photothermal approaches with the aid of curcumin photosensitizer and magnetic nanoparticles. *Sci Rep*. 2020;10:21206. doi:10.1038/s41598-020-78241-1
22. Manca ML, Matricardi P, Cencetti C, et al. Combination of argan oil and phospholipids for the development of an effective liposome-like formulation able to improve skin hydration and allantoin dermal delivery. *Int J Pharm*. 2016;505:204–211. doi:10.1016/j.ijpharm.2016.04.008
23. Sun Y, Deac A, Zhang GGZ. Assessing physical stability of colloidal dispersions using a turbiscan optical analyzer. *Mol Pharm*. 2019;16:877–885. doi:10.1021/acs.molpharmaceut.8b01194
24. Sentis MPL, Brambilla G, Fessard V, Meunier G. Simultaneous screening of the stability and dosimetry of nanoparticles dispersions for in vitro toxicological studies with static multiple light scattering technique. *Toxicol In Vitro*. 2020;69:104972. doi:10.1016/j.tiv.2020.104972
25. Dong W, Ye J, Wang W, et al. Self-Assembled Lecithin/Chitosan Nanoparticles Based on Phospholipid Complex: a Feasible Strategy to Improve Entrapment Efficiency and Transdermal Delivery of Poorly Lipophilic Drug. *Int J Nanomedicine*. 2020;15:5629–5643. doi:10.2147/IJN.S261162
26. Ye J, Yang Y, Jin J, et al. Targeted delivery of chlorogenic acid by mannosylated liposomes to effectively promote the polarization of TAMs for the treatment of glioblastoma. *Bioact Mater*. 2020;5:694–708. doi:10.1016/j.bioactmat.2020.05.001
27. Ye J, Li R, Yang Y, et al. Comparative colloidal stability, antitumor efficacy, and immunosuppressive effect of commercial paclitaxel nanoformulations. *J Nanobiotechnology*. 2021;19:199. doi:10.1186/s12951-021-00946-w
28. Zhang Y, Yang Y, Ye J, et al. Construction of chlorogenic acid-containing liposomes with prolonged antitumor immunity based on T cell regulation. *Sci China Life Sci*. 2021;64:1097–1115. doi:10.1007/s11427-020-1739-6
29. Katas H, Hussain Z, Awang SA. Bovine Serum Albumin-Loaded Chitosan/Dextran Nanoparticles: preparation and Evaluation of Ex Vivo Colloidal Stability in Serum. *J Nanomater*. 2013;2013:536291. doi:10.1155/2013/536291
30. Beijing Administration Rule of Laboratory Animals 2021; 2021. Available from: http://kwbeijinggovcn/art/2021/10/14/art_9220_625136html. Accessed December 1, 2022.
31. Urey C, Weiss VU, Gondikas A, et al. Combining gas-phase electrophoretic mobility molecular analysis (GEMMA), light scattering, field flow fractionation and cryo electron microscopy in a multidimensional approach to characterize liposomal carrier vesicles. *Int J Pharm*. 2016;513:309–318. doi:10.1016/j.ijpharm.2016.09.049
32. Jain AK, Thareja S. In vitro and in vivo characterization of pharmaceutical nanocarriers used for drug delivery. *Artif Cells Nanomed Biotechnol*. 2019;47:524–539. doi:10.1080/21691401.2018.1561457
33. Pochapski DJ, Carvalho Dos Santos C, Leite GW, Pulcinelli SH, Santilli CV. Zeta Potential and Colloidal Stability Predictions for Inorganic Nanoparticle Dispersions: effects of Experimental Conditions and Electrokinetic Models on the Interpretation of Results. *Langmuir*. 2021;37(45):13379–13389. doi:10.1021/acs.langmuir.1c02056
34. Shi C, Ahmad Khan S, Wang K, Schneider M. Improved delivery of the natural anticancer drug tetrandrine. *Int J Pharm*. 2015;479:41–51. doi:10.1016/j.ijpharm.2014.12.022
35. Carmona-Ribeiro AM. Biomimetic nanoparticles: preparation, characterization and biomedical applications. *Int J Nanomedicine*. 2010;5:249–259. doi:10.2147/IJN.S9035
36. Johansson E, Engvall C, Arfvidsson M, Lundahl P, Edwards K. Development and initial evaluation of PEG-stabilized bilayer disks as novel model membranes. *Biophys Chem*. 2005;113:183–192. doi:10.1016/j.bpc.2004.09.006
37. Johansson E, Lundquist A, Zuo S, Edwards K. Nanosized bilayer disks: attractive model membranes for drug partition studies. *Biochim Biophys Acta*. 2007;1768:1518–1525. doi:10.1016/j.bbamem.2007.03.006
38. Johnsson M, Edwards K. Liposomes, Disks, and Spherical Micelles: aggregate Structure in Mixtures of Gel Phase Phosphatidylcholines and Poly (Ethylene Glycol)-Phospholipids. *Biophys J*. 2003;85:3839–3847. doi:10.1016/S0006-3495(03)74798-5
39. Mahmoud NN, Abu-Dahab R, Abdallah M, et al. Interaction of gold nanorods with cell culture media: colloidal stability, cytotoxicity and cellular death modality. *J Drug Deliv Sci Technol*. 2020;60:101965. doi:10.1016/j.jddst.2020.101965
40. Argentiere S, Cella C, Cesaria M, Milani P, Lenardi C. Silver nanoparticles in complex biological media: assessment of colloidal stability and protein Corona formation. *J Nanopart Res*. 2016;18:253. doi:10.1007/s11051-016-3560-5
41. Madathiparambil Visalakshan R, González García LE, Benzigar MR, et al. The influence of nanoparticle shape on protein corona formation. *Small*. 2020;16:e2000285. doi:10.1002/smll.202000285
42. Yang M, Wu E, Tang W, Qian J, Zhan C. Interplay between nanomedicine and protein Corona. *J Mater Chem B*. 2021;9:6713–6727. doi:10.1039/D1TB01063H
43. Bilardo R, Traldi F, Vdovchenko A, Resmini M. Influence of surface chemistry and morphology of nanoparticles on protein Corona formation. *Wiley Interdiscip Rev Nanomed Nanobiotechnol*. 2022;14:e1788. doi:10.1002/wnan.1788
44. Chen T, Pan F, Luo G, et al. Morphology-driven protein Corona manipulation for preferential delivery of lipid nanodiscs. *Nano Today*. 2022;46:101609. doi:10.1016/j.nantod.2022.101609

45. Denisov IG, Sligar SG. Nanodiscs in membrane biochemistry and biophysics. *Chem Rev*. 2017;117:4669–4713. doi:10.1021/acs.chemrev.6b00690
46. Shao Q, Ding T, Pan F, et al. Protein corona mediated liposomal drug delivery for bacterial infection management. Asian J Pharmaceutical Sci. 2022;1:54.
47. Liu Y, Han Y, Fang T, et al. Turning weakness into strength: albumin nanoparticle-redirected amphotericin B biodistribution for reducing nephrotoxicity and enhancing antifungal activity. *J Control Release*. 2020;324:657–668. doi:10.1016/j.jconrel.2020.05.026
48. Marena GD, Ramos M, Bauab TM. A Critical Review of Analytical Methods for Quantification of Amphotericin B in Biological Samples and Pharmaceutical Formulations. *Crit Rev Anal Chem*. 2022;52:555–576. doi:10.1080/10408347.2020.1811947
49. Yang C, Xue B, Song W, et al. Reducing the toxicity of amphotericin B by encapsulation using methoxy poly(ethylene glycol)-b-poly(l-glutamic acid-co-l-phenylalanine). *Biomater Sci*. 2018;6:2189–2196. doi:10.1039/C8BM00506K